energies

MDPI

Article

Development and Evaluation of Newly Designed Coaxial Cylindrical Plasma Reactor with Liquid Flow Control and Post-Discharge Reactions for Water Treatment

Kosuke Tachibana [1], Ryosuke Hanabata [1,†], Takashi Furuki [1], Ryuta Ichiki [1], Seiji Kanazawa [1,*] and Marek Kocik [2]

[1] Department of Innovative Engineering, Oita University, 700 Dannoharu, Oita 870-1192, Japan; tachibana-kosuke@oita-u.ac.jp (K.T.); batate.6624@gmail.com (R.H.); furuki-takashi@oita-u.ac.jp (T.F.); ryu-ichiki@oita-u.ac.jp (R.I.)

[2] Institute of Fluid Flow Machinery, Polish Academy of Sciences, Fiszera 14, 80-231 Gdańsk, Poland; kocik@imp.gda.pl

* Correspondence: skana@oita-u.ac.jp; Tel.: +81-97-554-7828

† Current address: Kobe Works, Mitsubishi Electric Corporation, 1-1-2 Wadasaki-Cho, Kobe 652-8555, Japan.

Abstract: Water purification by non-equilibrium atmospheric pressure plasma has attracted much attention and is expected to be a next-generation method. However, general approaches to improve the energy efficiency of the water purification have not been revealed. Therefore, to investigate important factors for increasing its energy efficiency, we developed coaxial cylindrical plasma reactors where pulsed streamers were generated between a high-voltage electrode and running water film. To evaluate the performance of the plasma reactors, we measured hydroxyl (OH) radicals in solution based on a chemical probe method using disodium terephthalic acid (NaTA) and decolorized indigo carmine solution. Our experimental results showed that the production rate of the OH radicals was approximately 20 nmol/s and that the energy efficiency of the decolorization was on the order of 10 g/kWh. In addition, we found that controlling liquid flow based on the Coandă effect and introducing the intermittent operation of the streamer discharges to use post-discharge reactions increased the energy efficiency by a factor of approximately 3.5, which indicated that these approaches are effective to improve the performance of the water purification by plasma.

Keywords: non-equilibrium plasma; pulsed streamer; water film; OH radical; chemical probe method; Coandă effect; post-discharge reaction; water treatment

Citation: Tachibana, K.; Hanabata, R.; Furuki, T.; Ichiki, R.; Kanazawa, S.; Kocik, M. Development and Evaluation of Newly Designed Coaxial Cylindrical Plasma Reactor with Liquid Flow Control and Post-Discharge Reactions for Water Treatment. *Energies* **2022**, *15*, 4028. https://doi.org/10.3390/en15114028

Academic Editor: Keiichiro Yoshida

Received: 30 April 2022
Accepted: 27 May 2022
Published: 30 May 2022

1. Introduction

Recently, non-equilibrium atmospheric pressure plasma has been widely investigated for environmental, agricultural, and biomedical applications [1–3]. For example, Vasilev et al. decomposed organic compounds (solutes), such as phenol, caffeine, perfluorooctanoic acid (PFOA), and so on, in water by using pulsed plasmas generated over the water surface, and a rate-limiting step of the solutes' decomposition was investigated based on a mathematical model [4]. Griseti et al. irradiated an atmospheric pressure plasma jet to phosphate-buffered saline (PBS) and sodium chloride (NaCl) solutions, and it was found that the plasma-activated PBS was more suitable for killing cancer cells than the plasma-activated NaCl solution [5]. Nishimura et al. used a dielectric barrier discharge (DBD) to decompose ethylene gas, which was emitted from agricultural products and promoted their aging, so that fruits and vegetables were kept fresh [6]. Among these applications, we have paid attention to water purification by plasma as a next-generation method.

This is because non-equilibrium reaction fields can be used for the water purification by irradiating the non-equilibrium (non-thermal) plasma to the solution. In the plasma-induced reaction fields, we can use electrons with high energy, which is higher than that in

equilibrium (thermal) plasma, to generate reactive oxygen and nitrogen species (RONS) in the vicinity of the water surface, and these reactive species can be used to decompose persistent organic compounds in water [7]. For example, hydroxyl (OH) radicals, which are one of the RONS and have enough oxidizing power to decompose the persistent organic compounds, can be generated by the high-energy electrons through the following chemical reaction [8]:

$$H_2O + e^- \rightarrow OH + H. \quad (1)$$

We expected that, by using these characteristics and the chemical reactions, the non-equilibrium plasma can achieve the decomposition of the persistent organic compounds in water efficiently.

Although there are many researchers investigating the water purification by plasma, general approaches to improve its energy efficiency have not been revealed yet. Some papers reported that pulsed streamer discharge, which is one of the non-equilibrium plasmas, is more suitable for generating high-energy electrons. For example, Tomita et al. measured the velocity distribution of electrons generated by a pulsed positive streamer in air at atmospheric pressure with laser Thomson scattering, and it was found that the electron energy was a few eV and that the velocity distribution of the electrons deviated from that when they were in thermodynamic equilibrium (Maxwellian distribution) [9]. Other papers reported that flowing the treatment solution in contact with plasma was important to improve the energy efficiency. This is because the RONS generated by plasma, which are transported from the gas phase to the liquid phase, preferentially decompose the organic compounds in the vicinity of the plasma–liquid interface. Therefore, if the solution to which the plasma is irradiated does not have enough flow, the local concentrations of the organic compounds around the plasma–liquid interface can become very low, which leads to the decrease in the energy efficiency of the water treatment by plasma. Malik summarized the energy efficiency of the water purification by plasma [10], and it was found that high energy efficiency was achieved with plasma reactors where the treatment solution was flowed as droplets or water film [11,12].

In addition to using the pulsed streamers and controlling the water flow, we have focused on chemical reactions after the plasma is turned off (post-discharge reactions) as another approach to improve the energy efficiency of the water purification by plasma. Many researchers reported that plasma-activated or plasma-treated water (PAW or PTW), which is the solution to which the air plasma is irradiated, can retain the ability to kill bacteria after the plasma is turned off [13,14]. We believe that, if the post-discharge reactions can be used to decompose the persistent organic compounds in water, the energy efficiency of the water purification by plasma will be improved.

In order to evaluate the performance of the water purification by plasma, it is important to understand how much OH radicals are generated in solution. Although it is difficult to measure the OH radicals due to their short lifetime, there are some methods to estimate the OH radical concentrations in water, such as the electron spin resonance (ESR) method [15], the chemical probe method with coumarin [16], Fricke (ferrous sulfate ($FeSO_4$)) dosimetry [17], and so. A chemical probe method using terephthalic acid (TA) is also one of the methods to estimate the OH radical concentrations in water [18]. In this method, the TA reacts with the OH radicals to form 2-hydroxyterephthalic acid (HTA), and the OH radical concentrations are estimated based on the HTA concentrations, which are quantified by measuring HTA's fluorescence induced by UV-light irradiation. The advantage of this method is that expensive measurement equipment is not required and that the OH radicals in solution are selectively measured.

In this study, we developed new coaxial cylindrical-type reactors for the water purification by plasma. The performance of the new plasma reactors was evaluated based on OH radical measurements using a chemical probe method with disodium terephthalate (NaTA) and the decolorization characteristics of indigo carmine solution. To improve the energy efficiency of the decolorization, liquid flow control based on the Coandă effect [19–22] and intermittent operation of the streamer discharges to use post-discharge reactions were

introduced into our plasma reactors, and we investigated how these approaches influenced the performance of the decolorization by plasma. Based on our experimental results, we discuss what is important to improve the energy efficiency of the water purification by plasma.

2. Materials and Methods

In our experiments, we used two types of plasma reactors: an overflow-type reactor and a swirling-flow-type reactor, and their schematics are shown in Figure 1. Figure 1a shows the schematic of the overflow-type reactor. This reactor consisted of a quartz tube (14.5 mm in inner diameter and 300 mm in length) and acrylic vessels (bottom and top), and both ends of the quartz tube were connected with the acrylic vessels. Treatment solution was pumped up from the bottom to the top of the reactor with a peristaltic pump (Cole-Parmer Instrument, MasterFlex, models 7554-90 and 7518-10) and was gradually accumulated in the acrylic vessel (top). Then, when the solution exceeded the height of the quartz tube, the solution overflowed and fell down as water film along the inner wall of the quartz tube to the acrylic vessel (bottom). A threaded rod electrode (stainless steel, M4) was used as a high-voltage (H.V.) electrode and was located at the center of the quartz tube. A mesh electrode (stainless steel, 30 mesh) was employed as a grounded electrode and was wrapped around the outer wall of the quartz tube. A nanosecond-pulsed voltage provided from a pulsed power supply (Suematsu Electronics, MPC3010S-50SP) was applied to the H.V (threaded rod) electrode, and then, pulsed streamer discharges were generated between the threaded rod electrode and water film flowing along the inner wall of the quartz tube. It should be noted that the pulsed power supply, which was based on a magnetic pulse compression circuit, could generate the nanosecond-pulsed voltage, whose maximum peak voltage, typical pulse width (full width at half maximum (FWHM)), and maximum repetition frequency were 30 kV, 100 ns, and 500 pps, respectively. Output voltage waveforms of the pulsed power supply when the load was 300 Ω or 500 Ω are shown on the manufacturer's web page [23].

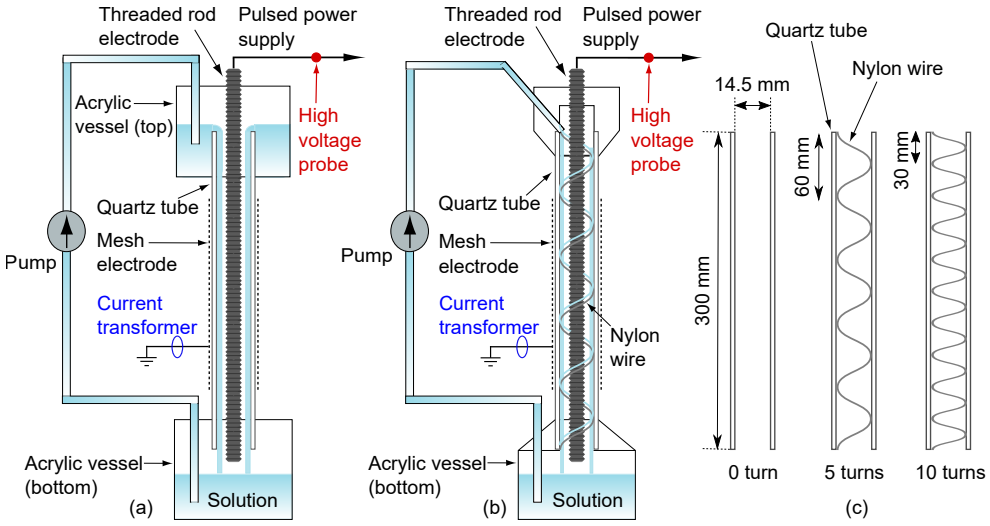

Figure 1. Schematics of coaxial cylindrical plasma reactors. (**a**) Overflow-type reactor. (**b**) Swirling-flow-type reactor. (**c**) Arrangement of nylon wire.

Figure 1b shows the schematic of the swirling-flow-type reactor. Its configuration was almost the same as that of the overflow-type reactor, but a spirally arranged nylon wire (0.8 mm in diameter) was added and located along the inner wall of the quartz tube. The specific arrangement of the nylon wire is shown in Figure 1c. In addition, at the top of the reactor, the treatment solution was ejected tangentially to the inner wall of the quartz tube so that the solution was able to propagate along the nylon wire on the inner wall of the quartz tube, leading to the generation of swirling water flow. This control of the

water flow was based on the Coandă effect, which explains the general tendency that fluid is likely to flow along the surface. We used the same pulsed power supply as used for the overflow-type reactor and irradiated the pulsed streamer discharges to the treatment solution in our experiments.

Because the nylon wire was added to the plasma generation area (inside of the quartz tube) of the reactor, there might be a concern about the possibility that the solution treated by plasma was possibly contaminated due the nylon wire. However, although the same nylon wire was used in the swirling-flow-type plasma reactor for a long time, changes of the nylon wire's conditions, such as surface roughness and color, could not be observed with the naked eye. (This was probably because the nylon wire was completely covered with the solution and did not contact the streamer discharges directly.) Therefore, it was expected that the solution after the streamer discharge irradiation was not contaminated.

The liquid flow running along the quartz tube and the pulsed streamer discharges generated between the threaded rod electrode and the water film were observed with a digital camera (Nikon (Tokyo, Japan), D5500). The pulsed streamers formed in one voltage pulse were captured with an intensified charge-coupled device (ICCD) camera (Andor Techonology (Belfast, Northern Ireland), iStar, DH734-18F-03). In measurements using the ICCD camera, its gate was synchronized with the streamer discharges by using a sync out signal of the pulsed power supply, and discharge images were captured in single-shot mode.

Voltage and current waveforms were captured with an oscilloscope (Yokogawa Electric (Tokyo, Japan), DML2024). The voltage across the H.V. (threaded rod) and the grounded (mesh) electrodes was measured with an H.V. probe (Iwatsu Electric (Tokyo, Japan), HV-P30), and the plasma current was monitored with a current transformer (Pearson Electronics (Palo Alto, CA, USA), model 4100). Energy consumption per pulse was obtained by using the following equation:

$$E = \int V \times I dt, \tag{2}$$

where E, V, and I are the energy consumption per pulse, applied voltage across the H.V. and the grounded electrodes, and the plasma current, respectively. The integration in Equation (2) was numerically calculated with a trapezoidal rule.

The temperature of the solution was measured under some experimental conditions before and after the plasma irradiation. In our experiments, the initial temperature of the solution was 20 ± 5 °C, and we confirmed that the solution's temperature after the streamer discharge irradiation was almost unchanged.

The OH radicals generated by the plasma in solution were estimated with the chemical probe method using NaTA (Tokyo Chemical Industry (Tokyo, Japan), T1097). In this method, the amount of OH radicals was estimated based on the concentrations of HTA, as well as the chemical probe method using TA. There are some papers reporting that a conversion rate of the NaTA to the HTA in the chemical reaction between the NaTA and the OH radicals was 35% [24,25]. Therefore, we calculated the amount of the OH radicals by using the following equation:

$$\text{Amount of OH} = \frac{100}{35} C_{\text{HTA}} V_0 \text{ [mol]}, \tag{3}$$

where C_{HTA} and V_0 are the HTA concentration and the volume of the treatment solution, respectively.

In our experiments, the HTA fluorescence at a wavelength of 425 nm was measured in two ways. In the first method, an in situ HTA fluorescence image was visualized by irradiating a UV lamp (Spectroline (Melville, NY, USA), EB-280CJ, wavelength: 312 nm) to the plasma reactor while the pulsed streamer discharges were generated. Although we could not identify the HTA concentrations, this method enabled us to observe the fluorescence image of the HTA. In the second method, the solution sample was taken from the plasma reactor and was put into a quartz cuvette (optical path length: 10 mm).

Then, the sample's fluorescence (425 nm), which was induced by a UV-LED light source (Sandhouse Design (Dunedin, FL, USA), LLS-310, wavelength: 310 nm), was measured with a UV-Vis spectrometer (Ocean Optics (Orlando, FL, USA), USB2000). A calibration curve for identifying the HTA concentrations was created with HTA solutions, which were prepared by dissolving solid HTA (Tokyo Chemical Industry, H1385) in distilled water.

Indigo carmine ($C_{18}H_8N_2Na_2O_8S_2$), which is a popular organic blue dye, was used for decolorization experiments to evaluate the performance of our plasma reactors. In these experiments, the indigo carmine solution was prepared by dissolving solid indigo carmine (FUJIFILM Wako Pure Chemical (Osaka, Japan), 090-00082) in distilled water and was circulated in the plasma reactors. Then, the pulsed streamer discharges were generated between the threaded rod electrode and the indigo carmine solution flowing along the inner wall of the quartz tube. The performance of our reactor was evaluated based on the decolorization rate, decolorization period, and energy efficiency. The decolorization rate indicated how much the blue color of the indigo carmine solution was decolorized by the plasma and was calculated based on the following equation:

$$\text{Decolorization rate} = \left(1 - \frac{A}{A_0}\right) \times 100\ [\%], \tag{4}$$

where A_0 and A are the absorbance of the indigo carmine solution before and during the experiments, respectively, at a wavelength of 610 nm. The absorbance of the indigo carmine solution was measured with a UV-Vis spectrometer (ASONE (Osaka, Japan), ASV11D). The decolorization period was defined as how long it took for the decolorization rate to become 95%. This was because, in our experiments, the decolorization was considered to be completed when the decolorization rate became more then 95%. The energy efficiency was defined as how much energy was consumed to achieve the 50% decolorization rate of the indigo carmine solution, which was calculated by the following equation:

$$G_{50} = 1.8 \times 10^3 \frac{C_0 V_0}{E f t_{50}} \quad [\text{g/kWh}], \tag{5}$$

where C_0, f, and t_{50} are the initial concentration of the indigo carmine, the pulse repetition frequency, and the duration of how long it took to decompose 50% indigo carmine in solution by plasma.

When we introduced the intermittent operation of the streamer discharges to use the post-discharge reactions in the decolorization experiments, the procedure of these experiments is described as follows:

1. Turned on the pulsed power supply, and generated the pulsed streamer discharges with a certain repetition frequency for t_{on}.
2. Turned off the pulsed power supply and kept the streamers off for t_{off}.
3. Took the solution sample and measured its absorbance at 610 nm.
4. Repeated Processes 1–3, which we call one cycle, until the decolorization rate became more than 95%.

In this procedure, t_{on} and t_{off} are defined as the on and off time of the streamer discharges in one cycle, respectively. It should be noted that the indigo carmine solution was circulated continuously during both t_{on} and t_{off}.

3. Results and Discussion

3.1. Flow and Discharge Characteristics

Figure 2 shows liquid flow propagating along the inner wall of the quartz tube in the swirling-flow-type reactor without and with the Coandă effect. In the latter case, the number of the nylon wire's turns was 10. The water flow was captured by using the digital camera with a frame rate of 60 fps. In these measurements, the indigo carmine solution was circulated with a flow rate of 1400 mL/min. In addition, the H.V. (threaded rod) and the grounded (mesh) electrodes were removed so that we were able to observe the liquid flow clearly.

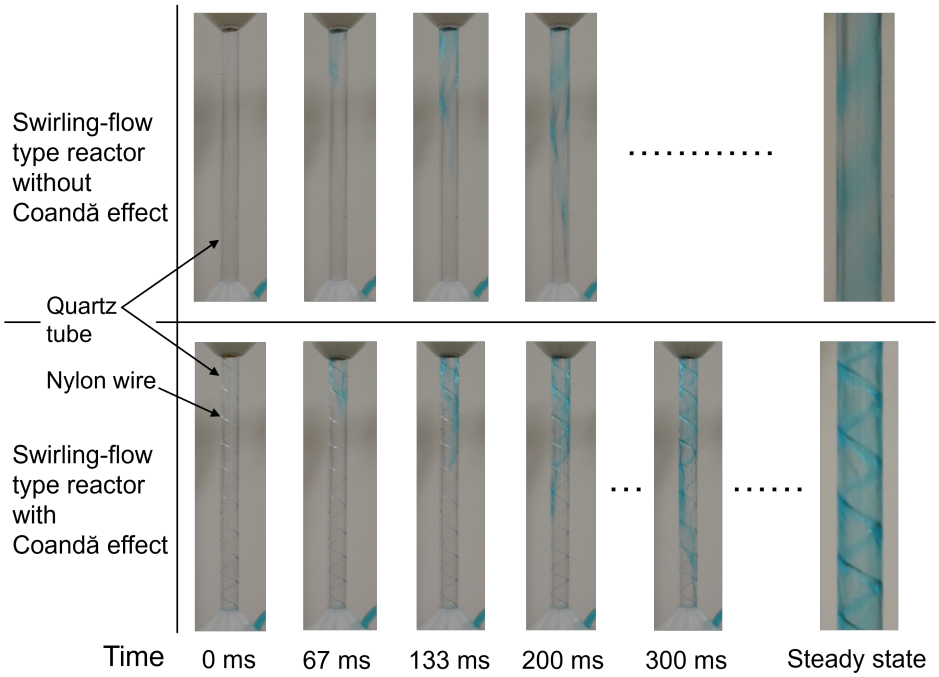

Figure 2. Liquid flow propagating along the inner wall of the quartz tube in the swirling-flow-type reactor without and with the Coandă effect. In the latter case, a spirally arranged nylon wire was used to make the swirling liquid flow based on the Coandă effect, and the number of turns was 10. The indigo carmine solution was circulated with a flow rate of 1400 mL/min, and its flow was captured by using a digital camera with a frame rate of 60 fps.

In the case of the swirling-flow-type reactor without the Coandă effect, the solution propagated from the top to the bottom along the quartz tube, and it took approximately 200 ms for the solution to pass the quartz tube. In the steady state, although the inner wall of the quartz tube was wholly covered with the solution, we observed that the shade of the blue color was different depending on the location. This observation indicated that the solution flow was not completely uniform because of the pulsation of the liquid flow caused by the peristaltic pump. The liquid flow observed in the swirling-flow-type reactor without the Coandă effect was almost the same as that observed in the overflow-type reactor. On the other hand, in the case of the swirling-flow-type reactor with the Coandă effect, the solution propagated along the spirally arranged nylon wire, which indicated that we achieved the control of the liquid flow by using the Coandă effect. In this case, it took approximately 300 ms for the solution to pass the quartz tube, which was longer than that in the overflow-type reactor by a factor of 1.5. This would be because the actual distance for the solution to pass the quartz tube in the swirling-flow-type reactor was longer than that in the overflow-type reactor. In the steady state, we confirmed that the inner wall of the quartz tube was wholly covered with the solution.

Figure 3 shows typical voltage and current waveforms when the pulsed streamer discharges were generated between the H.V. (threaded rod) electrode and the water film in the overflow-type reactor. In this measurement, the streamer discharges were driven by the nanosecond-pulsed voltage with a peak value and a repetition frequency of 24 kV and 100 pps, respectively. As shown in Figure 3, the peak value and the pulse width of the current were approximately 50 ns and 100 A, respectively. In addition, it was found that the pulse width (FWHM) of the voltage waveform was approximately 150 ns, which was a little different from the typical pulse width (100 ns) provided by the manufacturer, probably due to a difference of the load. The energy consumption per pulse, which was calculated based on Equation (2), was approximately 70 mJ. Therefore, the power consumption of the pulsed streamer discharges was approximately 7.0 W.

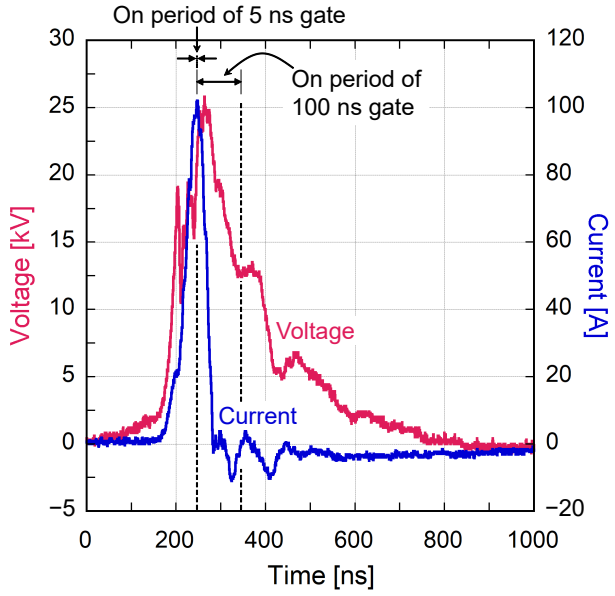

Figure 3. Typical voltage and current waveforms when pulsed streamer discharges were generated in the overflow-type reactor. These discharges were driven by nanosecond-pulsed voltages whose peak value and repetition frequency were 24 kV and 100 pps, respectively. Time relationship between the gate of an intensified charge-coupled device (ICCD) camera and voltage and current waveforms is also shown to indicate when the streamer discharges were captured by the ICCD camera in Figure 4.

Figure 4 shows pulsed streamers captured by the ICCD camera with exposure times of 5 ns (Figure 4a) and 100 ns (Figure 4b) for the overflow-type reactor. In the case of the 5 ns exposure time, we adjusted the gate of the ICCD camera so that the streamer discharges when the current became maximum were able to be observed. On the other hand, in the case of the 100 ns exposure time, the gate of the ICCD camera opened when the current became maximum, and the image of the streamer discharges was recorded for 100 ns. The time relationship between the gate of the ICCD camera and the voltage and current waveforms is shown in Figure 3. The pulsed streamers were generated by nanosecond-pulsed voltage with a peak value of 24 kV and a repetition frequency of 100 pps while tap water was circulated with a flow rate of 500 mL/min. In these measurements, the mesh electrode was partly removed from the quartz tube so that we were able to observe the pulsed streamers clearly. As shown in Figure 4a, the pulsed streamers bridged the gap (approximately 5 mm) between the threaded rod electrode and the water surface within 5 ns, which indicated that the propagation speed of the pulsed streamers was at least 5 mm/5 ns $= 1 \times 10^6$ m/s. Furthermore, from Figure 4b, we estimated the diameter of the streamer channels to be 0.2–0.5 mm. The propagation speed and the diameter of the pulsed streamers were similar to those reported by other researchers, which were on the order of 10^5–10^6 m/s and 0.1 mm, respectively [26,27]. Both Figure 4a,b show that the many filamentary streamers were generated between the threaded rod electrode and the water film over the wide region.

Figure 5 shows discharge images taken by the digital camera with an exposure time of 10 s for the swirling-flow-type reactor without and with the Coandă effect (number of nylon wire turns: 10). The streamer discharges were generated by the nanosecond-pulsed voltage, whose peak value and repetition frequency were 27 kV and 100 pps, respectively. As shown in both Figure 5a,b, the pulsed streamer discharges were generated over the whole region of the quartz tube in both the overflow- and swirling-flow-type reactors. It should be noted the streamer discharges observed in the swirling-flow-type reactor without the Coandă effect were almost the same as those observed in the overflow-type reactor.

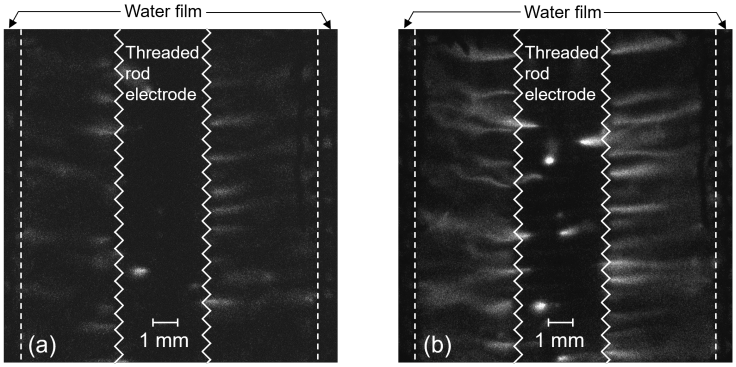

Figure 4. Pulsed streamer discharges taken by an intensified charge-coupled device (ICCD) camera. (**a**) Exposure time: 5 ns. (**b**) Exposure time: 100 ns. The pulsed streamers were driven by nanosecond-pulsed voltage, whose peak value and repetition frequency were 24 kV and 100 pps, respectively, while tap water was circulated with a flow rate of 500 mL/min.

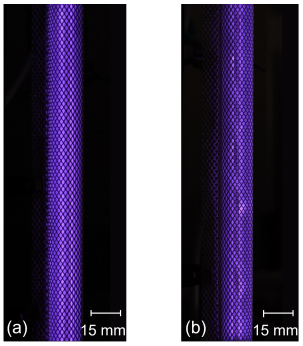

Figure 5. Discharge images taken by a digital camera with an exposure time of 10 s. (**a**) Swirling-flow-type reactor without the Coandă effect. (**b**) Swirling-flow-type reactor with the Coandă effect (number of nylon wire turns: 10). The streamer discharges were generated by the nanosecond-pulsed voltage, whose peak value and repetition frequency were 27 kV and 100 pps, respectively, while the solution was circulated with a flow rate of 1400 mL/min.

3.2. Measurement of OH Radicals in Solution with Chemical Probe Method Using NaTA

Figure 6 shows a typical in situ fluorescence image of the HTA when we irradiated the pulsed streamers to the 2 mM NaTA solution in the overflow-type reactor. The streamer discharges were generated by the nanosecond-pulsed voltage, whose peak value and repetition frequency were 24 kV and 100 pps, respectively, and the HTA fluorescence (425 nm) was induced by the UV lamp with a wavelength of 312 nm. As shown in Figure 6, we observed the blue fluorescence of the HTA, which indicated that the OH radicals were generated by pulsed streamer discharges and reacted with the NaTA to form the HTA. As time elapsed, the blue fluorescence of the HTA became bright enough for us to observe it with the naked eye.

Figure 7 shows the estimated amount of the OH radicals in solution as a function of treatment time with various volumes of 2 mM NaTA solutions. The streamer discharges were generated by pulsed voltage with a peak value and a repetition frequency of 24 kV and 100 pps, respectively, and were irradiated to the 2 mM NaTA solution in the overflow-type reactor. The 2 mM NaTA solution was circulated with a flow rate of 600 mL/min, and the amount of OH radicals in solution was estimated based on Equation (3). According to Figure 7, the amount of OH radicals in the solution increased almost linearly until the treatment time became 300 s. However, the increase in the amount of OH radicals gradually decayed after 300 s, and this decay became more remarkable as the volume of the 2 mM NaTA solution decreased from 1000 mL to 220 mL. In the case of the 220 mL volume,

the estimated amount of the OH radicals in solution leveled off after the pulsed streamers were irradiated for approximately 600 s.

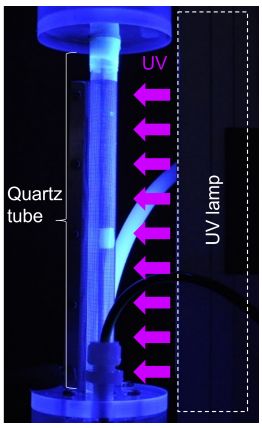

Figure 6. Typical in situ fluorescence image of 2-hydroxyterephthalic acid (HTA) induced by UV-light irradiation. The streamer discharges were generated by nanosecond-pulsed voltage whose peak value and repetition frequency were 24 kV and 100 pps, respectively, and were irradiated to the 2 mM disodium terephthalate (NaTA) solution.

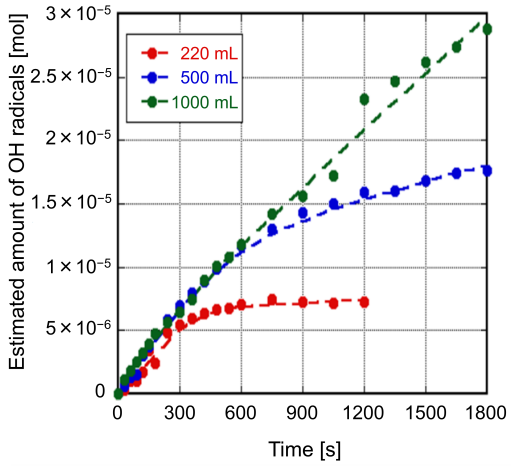

Figure 7. Estimated amount of OH radicals in the solution as a function of time with various volumes of 2 mM NaTA solution. Pulsed streamer discharges with a peak value and repetition frequency of 24 kV and 100 pps were irradiated to the 2 mM NaTA solution, which was circulated with a flow rate of 600 mL/min.

The decay of the increase in the estimated amount of the OH radicals after the 300 s treatment time would be caused by the HTA decomposition by the plasma. Shiraki et al. reported that, when pulsed plasmas were irradiated to a 2 mM NaTA solution for 600 s, the HTA concentrations increased until 300 s, but decreased after 300 s [28]. To explain this decrease in the HTA concentrations, they proposed HTA decomposition by the OH radicals based on their experiments and numerical simulations. We believe that the same HTA decomposition would happen in our experiments, and therefore, the decay of the estimated OH radicals would not be caused by the decrease in the OH radical production, but the decomposition of the HTA.

Considering the HTA decomposition by OH radicals, only the OH radicals measured before 300 s were reliable. Therefore, we calculated the production rate of the OH radicals using the measured values before 300 s, and the calculated production rate was approximately 20 nmol/s. We found that this value was higher than that of pulsed streamer discharges in liquid [29].

3.3. Decolorization Characteristics

Figure 8 shows decolorization rates as a function of time with various peak values of the applied pulsed voltages. In these decolorization experiments, the pulsed streamer discharges were irradiated to the 10 mg/L indigo carmine solution in the overflow-type reactor. The repetition rate of the pulsed voltage was 100 pps, and the indigo carmine solution was circulated with a flow rate of 600 mL/min. When the peak voltage increased from 18 kV to 21 kV, the decolorization rate increased quickly and the decolorization period became shorter by approximately 30 s. However, when we increased the peak voltage more than 21 kV, the temporal changes of the decolorization rates or the decolorization periods did not vary very much. These results indicated that, as the peak value of the pulsed voltage became higher than 21 kV, more radicals generated by the pulsed streamers were wasted without reacting with the indigo carmine, leading to the lesser energy efficiency (G_{50}) of the decolorization.

The contribution of the OH radicals to the decolorization was estimated based on the following assumptions:

- All the OH radicals shown in Figure 7 were used to decompose the indigo carmine.
- The reaction between one OH radical and one indigo carmine molecule always led to the decolorization.

These assumptions enabled us to evaluate the possible maximum contribution of the OH radicals to the decolorization. According to Figure 8, the decolorization rate with a 24 kV peak voltage at 120 s was 92.6%, and therefore, the amount of the indigo carmine decomposed by plasma was 4.37 µmol (=10 mg/L × 220 mL × 0.926 ÷ 466.36 g/mol). On the other hand, since the production rate of the OH radicals, which was estimated based on Figure 7, was 20 nmol/s, the amount of the OH radicals generated by the plasma in the solution was 2.40 µmol (=20 nmol/s × 120 s). Thus, the possible maximum contribution of the OH radicals to the decolorization was estimated to be approximately 55% (2.40 µmol ÷ 4.37 µmol × 100).

Figure 9 shows the decolorization rates of the 10 mg/L indigo carmine solution as a function of treatment time with various turns of the nylon wire. The indigo carmine solution, which was circulated with a flow rate of 1400 mL/min, was decolorized by the pulsed streamer discharges with a peak voltage and a repetition frequency of 21 kV and 100 pps, respectively, in the swirling-flow-type reactor. According to Figure 9, the decolorization rates increased rapidly more as the number of the nylon wire turns became larger. We also found that the decolorization period for 10 turns was 60 s, which was half of that for 0 turns. Furthermore, it was confirmed that the decolorization rates for the swirling-flow-type reactor without the Coandă effect (number of the nylon wire turns: 0) were almost the same as those for the overflow-type reactor.

The increase in the speed of the decolorization by adding the nylon wire to the plasma reactor could be caused by the improvement of the liquid flow, which led to the enhancement of the transportation and mixing of the reactive species including the OH radicals and the indigo carmine. As shown in Figure 2, we achieved the swirling water flow by locating the spirally arranged nylon wire along the inner wall of the quartz tube of the plasma reactor, and this swirling flow would be enhanced by increasing the number of nylon wire turns. This swirling liquid flow probably promoted the transportation and mixing of the reactive species and the indigo carmine around the plasma–liquid interface, and therefore, the reactive species would be able to decolorize the indigo carmine solution more effectively, which led to the higher decolorization rates with the number of nylon wire turns. It should be noted that almost no changes were observed in the streamer discharges when the nylon wire was added to the plasma reactor. Therefore, it was expected that the amount of the OH radicals generated by the plasma would not be changed depending on the turn number of the nylon wire.

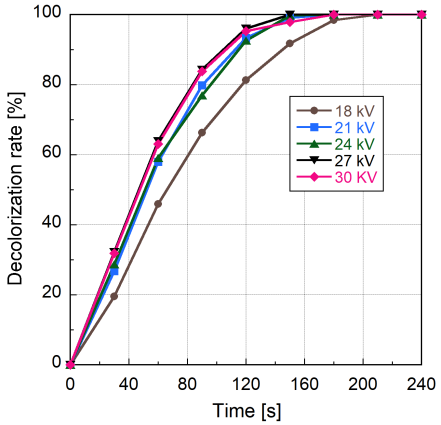

Figure 8. Decolorization rates of indigo carmine as a function of treatment time with various peak values of applied pulsed voltage. Pulsed streamer discharges with a repetition frequency of 100 pps were irradiated to the 10 mg/L indigo carmine solution in the overflow-type reactor. The solution was circulated with a flow rate of 600 mL/min.

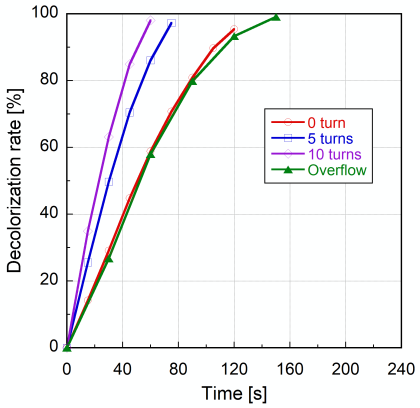

Figure 9. Decolorization rates of indigo carmine as a function of treatment time with various turns of the nylon wire (0.8 mm in diameter). Pulsed streamer discharges with the peak voltage and repetition frequency of 21 kV and 100 pps were irradiated to the 10 mg/L indigo carmine solution in the swirling-flow-type reactor. The solution was circulated with a flow rate of 1400 mL/min.

Figure 10 shows the decolorization rates of indigo carmine as a function of time when we introduced the intermittent operation of the streamer discharges (t_{on} and t_{off}) to use the post-discharge reactions in the decolorization experiments. In these experiments, the 10 mg/L indigo carmine solution was circulated continuously with a flow rate of 1400 mL/min and was decolorized by pulsed streamers with a peak voltage and a repetition frequency of 21 kV and 100 pps, respectively, during t_{on}. As shown in Figure 10, although introducing t_{off} made the decolorization periods longer, the decolorization rates after each cycle were increased. These results indicate that the indigo carmine solution was decolorized by the post-discharge reactions while the streamer discharges were kept off.

Possible reactions occurring during t_{off} would be the same as those occurring in the plasma-treated water (PTW). The reaction processes of the PTW were proposed by Ikawa et al. and are described as the following chemical reactions [30]:

$$NO_2^- + H_2O_2 \rightarrow ONOO^- + H_2O \quad (6)$$

$$ONOO^- + H_2O_2 \rightarrow O_2NOO^- + H_2O \quad (7)$$

$$O_2NOO^- \leftrightarrow O_2^- + NO_2 \quad (8)$$

Because it is known that streamer discharges generated in air can form nitrite ions (NO_2^-) and hydrogen peroxide (H_2O_2) [31], peroxynitrite ($ONOO^-$) and peroxynitric ions

(O_2NOO^-) can be generated through the reactions (6) and (7). Therefore, superoxide ions (O_2^-) formed through the reactions (8) are probably responsible for decolorizing the indigo carmine solution in our experiments.

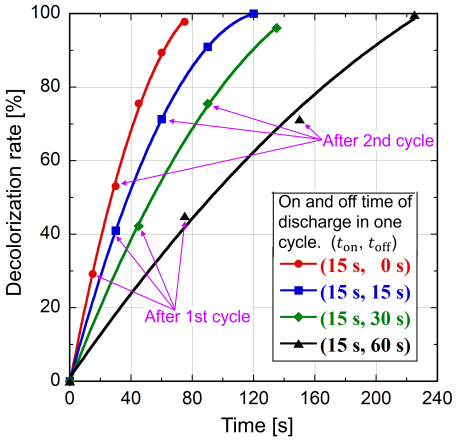

Figure 10. Decolorization rate of indigo carmine as a function of treatment time when intermittent operation was introduced to use post-discharge reactions. t_{on} and t_{off} are defined as the on and off time of the streamer discharges in one cycle, which consisted of turning on the discharge, turning off the discharge, and measuring the absorbance of treatment solution. The 10 mg/L indigo carmine solution was decolorized by the streamer discharges, whose peak voltage and repetition frequency were 21 kV and 100 pps, respectively. The solution was circulated continuously with a flow rate of 1400 mL/min during the experiments.

There are some papers reporting the decomposition process of the indigo carmine caused by the O_2^- ions and the OH radicals. For example, Kettle et al. investigated the by-products of the indigo carmine when it was decomposed with O_2^- ions generated by a chemical method [32]. They found that O_2^- ions were able to decompose the indigo carmine by breaking its C=C bond and that isatin 5-sulfonic acid ($C_8H_4NNaO_5S$) was generated. Flox et al. decomposed the indigo carmine in acidic aqueous solution by a chemical method, and it was found that the OH radicals were able to break the C=C bond of the indigo carmine and that, in addition to the isatin 5-sulfonic acid, indigo ($C_{16}H_{10}N_2O_2$) and isatin ($C_8H_5NO_2$) were generated [33]. Crema et al. used an atmospheric pressure plasma generated over the water surface in oxygen or nitrogen gas to decompose the indigo carmine in solution, and its by-products were identified as the isatin 5-sulfonic acid, isatin, indole (C_8H_7N), and so on [34]. Because the OH radicals and the O_2^- ions are expected to primarily decompose the indigo carmine in our experiments, the similar decomposition process of the indigo carmine introduced above probably occurred, and similar by-products might be generated after the decolorization experiments.

Although we did not measure the intensity of ultraviolet (UV) light emitted from the plasma, the UV light might be able to decolorize the indigo carmine solution. For example, Lukes et al. measured intensity of UV radiation emitted from underwater plasma, and the UV radiation can play an important role in bacterial inactivation and the generation of hydrogen peroxide [35]. Tian et al. performed a numerical simulation of dielectric barrier discharges generated in humid air, and it was found that UV/VUV radiation derived from excited nitrogen species played a significant role in producing the OH radicals [36]. The investigation about the contribution of the UV light to the decolorization of the indigo carmine solution is out of the scope of this paper, but will be addressed in future work.

Figure 11 shows a comparison of the energy efficiency G_{50} of the indigo carmine decomposition when we introduced the liquid flow control based on the Coandă effect and the post-discharge reactions in the plasma reactors. G_{50} increased from 11.5 g/kWh to 30.5 g/kWh by locating the spirally arranged nylon wire along the inner wall of the quartz tube. In our experiments, the energy efficiency G_{50} was the highest when the number

of nylon wire turns was 10, but it might be possible to obtain a higher G_{50} by increasing the number of turns. Figure 11 also shows that introducing the off time of the streamer discharges increased the energy efficiency G_{50} from 30.5 g/kWh to 41.0 g/kWh. This would be because the indigo carmine solution was decolorized through post-discharge reactions during t_{off}. From Figure 11, we found that the 30 s off time of the streamer discharges in one cycle was enough to use the post-discharge reactions effectively. We also observed that introducing both the Coandă effect and the post-discharge reactions improved the G_{50} by approximately 3.5 times (from 11.5 g/kWh to 40.5 g/kWh).

Our experimental results indicate that the liquid flow control based on the Coandă effect and the intermittent operation of the streamer discharges to use the post-discharge reactions are effective to improve the performance of the plasma reactor. Although there are some papers reporting higher energy efficiencies G_{50} compared with those in our experiments [11,12], what we found in this study is very valuable to improve the performance of plasma reactors.

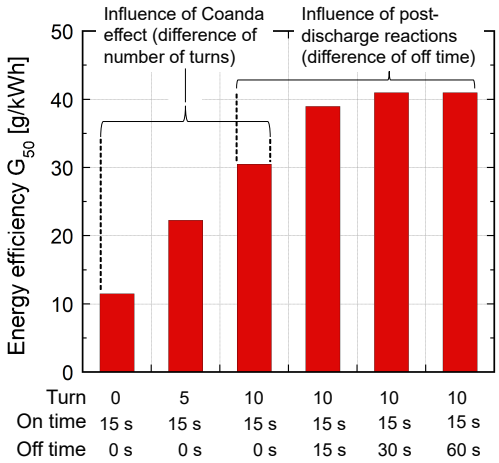

Figure 11. Comparison of the energy efficiency G_{50} of indigo carmine decolorization when the Coandă effect and post-discharge reactions were introduced in our plasma reactors.

4. Conclusions

We developed new coaxial cylindrical reactors for water purification by plasma. The plasma reactors consisted of a quartz tube and acrylic vessels, and the treatment solution flowed along the inner wall of the quartz tube from top to bottom. Then, the pulsed streamer discharges were generated between a high-voltage electrode and running water film. To evaluate the performance of the newly developed plasma reactors, we measured hydroxyl (OH) radicals in solution by using a chemical probe method with disodium terephthalic acid (NaTA) and decolorized indigo carmine solution.

The measurements of the OH radicals indicated that the production rate of the OH radicals in our plasma reactor was approximately 20 nmol/s. In our experiments, more than a 95% decolorization rate of the indigo carmine solution was achieved within 180 s in most cases, and the energy efficiency, which is defined as how much energy was consumed to achieve the 50% decolorization rate of the indigo carmine solution, was on the order of 10 g/kWh. The energy efficiency increased by a factor of approximately 3.5 by introducing liquid flow control based on the Coandă effect and intermittent operation of the streamer discharges to use post-discharge reactions, which indicated that these approaches are effective to improve the performance of the water purification by plasma.

Author Contributions: Conceptualization, S.K.; methodology, S.K. and M.K.; investigation, K.T., R.H. and T.F.; data curation, K.T., R.H., T.F. and S.K.; writing—original draft preparation, K.T.; writing—review and editing, K.T., R.H., T.F., R.I., S.K. and M.K.; supervision, K.T, R.I., S.K. and M.K.; funding acquisition, S.K. All authors have read and agreed to the published version of the manuscript.

Funding: This work was supported by JSPS KAKENHI (A) Grant Number 17H01257.

Institutional Review Board Statement: Not applicable.

Informed Consent Statement: Not applicable.

Data Availability Statement: The data presented in this study are available upon request from the corresponding author.

Conflicts of Interest: The authors declare no conflict of interest.

References

1. Locke, B.R. Environmental applications of electrical discharge plasma with liquid water: A mini review. *Int. J. Plasma Environ. Sci. Technol.* **2012**, *6*, 194–203.
2. Kong, M.G.; Kroesen, G.; Morfill, G.; Nosenko, T.; Shimizu, T.; Van Dijk, J.; Zimmermann, J.L. Plasma medicine: An introductory review. *New J. Phys.* **2009**, *11*, 115012. [CrossRef]
3. Šimek, M.; Homola, T. Plasma-assisted agriculture: History, presence, and prospects-a review. *Eur. Phys. J. D* **2021**, *75*, 210. [CrossRef]
4. Vasilev, M.; Conlon, P.; Bohl, D.; Thagard, S.M. The Effect of Discharge Frequency of a Gas–Liquid Plasma Reactor on Bulk Liquid Transport and Removal of Organic Contaminants. *Plasma Chem. Plasma Process.* **2022**, 1–25. [CrossRef]
5. Griseti, E.; Merbahi, N.; Golzio, M. Anti-cancer potential of two plasma-activated liquids: Implication of long-lived reactive oxygen and nitrogen species. *Cancers* **2020**, *12*, 721. [CrossRef] [PubMed]
6. Nishimura, J.; Takahashi, K.; Takaki, K.; Koide, S.; Suga, M.; Orikasa, T.; Teramoto, Y.; Uchino, T. Removal of ethylene and by-products using dielectric barrier discharge with Ag nanoparticle-loaded zeolite for keeping freshness of fruits and vegetables. *Trans. Mater. Res. Soc. Jpn.* **2016**, *41*, 41–45. [CrossRef]
7. Bruggeman, P.J.; Kushner, M.J.; Locke, B.R.; Gardeniers, J.G.E.; Graham, W.G.; Graves, D.B.; Hofman-Caris, R.; Maric, D.; Reid, J.P.; Ceriani, E.; et al. Plasma–liquid interactions: A review and roadmap. *Plasma Sources Sci. Technol.* **2016**, *25*, 53002. [CrossRef]
8. Itikawa, Y.; Nigel, M. Cross Sections for Electron Collisions with Water Molecules. *J. Phys. Chem. Ref. Data* **2005**, *34*, 1–22. [CrossRef]
9. Tomita, K.; Inada, Y.; Komuro, A.; Zhang, X.; Uchino, K.; Ono, R. Measurement of electron velocity distribution function in a pulsed positive streamer discharge in atmospheric-pressure air. *J. Phys. D Appl. Phys.* **2019**, *53*, 08LT01. [CrossRef]
10. Malik, M.A. Water purification by plasmas: Which reactors are most energy efficient? *Plasma Chem. Plasma Process.* **2010**, *30*, 21–31. [CrossRef]
11. Minamitani, Y.; Shoji, S.; Ohba, Y.; Higashiyama, Y. Decomposition of dye in water solution by pulsed power discharge in a water droplet spray. *IEEE Trans. Plasma Sci.* **2008**, *36*, 2586–2591. [CrossRef]
12. Yano, T.; Uchiyama, I.; Fukawa, F.; Teranishi, K.; Shimomura, N. Water treatment by atmospheric discharge produced with nanosecond pulsed power. In Proceedings of the 2008 IEEE International Power Modulators and High-Voltage Conference, Las Vegas, NV, USA, 27–31 May 2008; pp. 80–83.
13. Tanaka, H.; Mizuno, M.; Ishikawa, K.; Nakamura, K.; Kajiyama, H.; Kano, H.; Kikkawa, F.; Hori, M. Plasma-activated medium selectively kills glioblastoma brain tumor cells by down-regulating a survival signaling molecule, AKT kinase. *Plasma Med.* **2011**, *1*, 265–277. [CrossRef]
14. Ikawa, S.; Kitano, K.; Hamaguchi, S. Effects of pH on bacterial inactivation in aqueous solutions due to low-temperature atmospheric pressure plasma application. *Plasma Process. Polym.* **2010**, *7*, 33–42. [CrossRef]
15. Tani, A.; Ono, Y.; Fukui, S.; Ikawa, S.; Kitano, K. Free radicals induced in aqueous solution by non-contact atmospheric-pressure cold plasma. *Appl. Phys. Lett.* **2012**, *100*, 254103. [CrossRef]
16. Jean-M, F.; Xochitl, D.B.; Mika, S.; Others. Towards reliable quantification of hydroxyl radicals in the Fenton reaction using chemical probes. *RSC Adv.* **2018**, *8*, 5321–5330.
17. Mark, G.; Tauber, A.; Laupert, R.; Schuchmann, H.P.; Schulz, D.; Mues, A.; von Sonntag, C. OH-radical formation by ultrasound in aqueous solution–Part II: Terephthalate and Fricke dosimetry and the influence of various conditions on the sonolytic yield. *Ultrason. Sonochem.* **1998**, *5*, 41–52. [CrossRef]
18. Kanazawa, S.; Kawano, H.; Watanabe, S.; Furuki, T.; Akamine, S.; Ichiki, R.; Ohkubo, T.; Kocik, M.; Mizeraczyk, J. Observation of OH radicals produced by pulsed discharges on the surface of a liquid. *Plasma Sources Sci. Technol.* **2011**, *20*, 34010. [CrossRef]
19. Coanda, H. Propulseur. France Patent 416541, 22 October 1910.
20. Coanda, H. Propeller. U.S. Patent 1,104,963, 28 July 1914.
21. Coanda, H. Device for Deflecting a Stream of Elastic Fluid Projected into an Elastic Fluid. U.S. Patent 2,052,869, 1 September 1936.
22. Reba, I. Applications of the Coanda effect. *Sci. Am.* **1966**, *214*, 84–93. [CrossRef]
23. Suematsu Electronics. MPC Series | High Voltage, High Power, High Repetition Rate. Available online: http://www.suematsu-el.jp/en/products/02.php (accessed on 22 May 2022) .
24. Matthews, R.W. The radiation chemistry of the terephthalate dosimeter. *Radiat. Res.* **1980**, *83*, 27–41. [CrossRef]
25. Fang, X.; Mark, G.; von Sonntag, C. OH radical formation by ultrasound in aqueous solutions Part I: The chemistry underlying the terephthalate dosimeter. *Ultrason. Sonochem.* **1996**, *3*, 57–63. [CrossRef]

26. Ono, R.; Oda, T. Formation and structure of primary and secondary streamers in positive pulsed corona discharge-effect of oxygen concentration and applied voltage. *J. Phys. D Appl. Phys.* **2003**, *36*, 1952. [CrossRef]
27. Namihira, T.; Wang, D.; Katsuki, S.; Hackam, R.; Akiyama, H. Propagation velocity of pulsed streamer discharges in atmospheric air. *IEEE Trans. Plasma Sci.* **2003**, *31*, 1091–1094. [CrossRef]
28. Shiraki, D.; Ishibashi, N.; Takeuchi, N. Quantitative Estimation of OH Radicals Reacting in Liquid Using a Chemical Probe for Plasma in Contact With Liquid. *IEEE Trans. Plasma Sci.* **2016**, *44*, 3158–3163. [CrossRef]
29. Kanazawa, S.; Furuki, T.; Nakaji, T.; Akamine, S.; Ichiki, R. Application of chemical dosimetry to hydroxyl radical measurement during underwater discharge. In *Journal of Physics: Conference Series, Proceedings of the 7th International Conference on Applied Electrostatics (ICAES-2012), Dalian, China, 17–19 September 2012*; IOP Publishing: Bristol, UK, 2013 ; Volume 418, p. 12102.
30. Ikawa, S.; Tani, A.; Nakashima, Y.; Kitano, K. Physicochemical properties of bactericidal plasma-treated water. *J. Phys. D. Appl. Phys.* **2016**, *49*, 425401. [CrossRef]
31. Lukes, P.; Dolezalova, E.; Sisrova, I.; Clupek, M. Aqueous-phase chemistry and bactericidal effects from an air discharge plasma in contact with water: Evidence for the formation of peroxynitrite through a pseudo-second-order post-discharge reaction of H_2O_2 and HNO_2. *Plasma Sources Sci. Technol.* **2014**, *23*, 15019. [CrossRef]
32. Kettle, A.J.; Clark, B.M.; Winterbourn, C.C. Superoxide converts indigo carmine to isatin sulfonic acid: implications for the hypothesis that neutrophils produce ozone. *J. Biol. Chem.* **2004**, *279*, 18521–18525. [CrossRef]
33. Flox, C.; Ammar, S.; Arias, C.; Brillas, E.; Vargas-Zavala, A.V.; Abdelhedi, R. Electro-Fenton and photoelectro-Fenton degradation of indigo carmine in acidic aqueous medium. *Appl. Catal. B Environ.* **2006**, *67*, 93–104. [CrossRef]
34. Crema, A.P.S.; Borges, L.D.P.; Micke, G.A.; Debacher, N.A. Degradation of indigo carmine in water induced by non-thermal plasma, ozone and hydrogen peroxide: A comparative study and by-product identification. *Chemosphere* **2020**, *244*, 125502. [CrossRef]
35. Lukes, P.; Clupek, M.; Babicky, V.; Sunka, P. Ultraviolet radiation from the pulsed corona discharge in water. *Plasma Sources Sci. Technol.* **2008**, *17*, 24012. [CrossRef]
36. Tian, W.; Kushner, M.J. Atmospheric pressure dielectric barrier discharges interacting with liquid covered tissue. *J. Phys. D Appl. Phys.* **2014**, *47*, 165201. [CrossRef]